Microchimica Acta (2024) 191:418
https://doi.org/10.1007/s00604-024-06469-z

ORIGINAL PAPER

An electrochemical immunosensor based on MXene-GQD/AuNPs for the detection of trace amounts of CA-125 as specific tracer of ovarian cancer

Zahra Hosseinchi Gharehaghaji[1,2] · Balal Khalilzadeh[3,4] · Hadi Yousefi[5] · Rahim Mohammad-Rezaei[2]

Received: 29 February 2024 / Accepted: 26 May 2024 / Published online: 24 June 2024

Abstract

An electrochemical immunoassay system was developed to detect CA-125 using a glassy carbon electrode (GCE) modified with MXene, graphene quantum dots (GQDs), and gold nanoparticles (AuNPs). The combined MXene-GQD/AuNPs modification displayed advantageous electrochemical properties due to the synergistic effects of MXene, GQDs, and AuNPs. The MXene-GQD composite in the modified layer provided strong mechanical properties and a large specific surface area. Furthermore, the presence of AuNPs significantly improved conductivity and facilitated the binding of anti-CA-125 on the modified GCE, thereby enhancing sensitivity. Various analytical techniques such as FE-SEM and EDS were utilized to investigate the structural and morphological characteristics as well as the elemental composition. The performance of the developed immunosensor was assessed using electrochemical impedance spectroscopy (EIS), cyclic voltammetry (CV), square wave voltammetry (SWV), and differential pulse voltammetry (DPV). Under optimized conditions in a working potential range of −0.2 to 0.6 V (vs. Ag/AgCl), the sensitivity, linear range (LR), limit of detection (LOD), and correlation coefficient (R^2) were determined to be 315.250 μA pU.mL^{-1}/cm^2, 0.1 to 1 nU/mL, 0.075 nU/mL, and 0.9855, respectively. The detection of CA-125 in real samples was investigated using the developed immunoassay platform, demonstrating satisfactory results including excellent selectivity and reproducibility.

Keywords Electrochemical immunosensor · Modified glassy carbon electrode · MXene · Ovarian cancer · Cancer antigen-125 detection · Graphene quantum dots

Introduction

Women with gynecologic malignancies are mostly affected by ovarian cancer (OC). In recent decades, the death rate from OC has not decreased much, despite all the advances in cancer treatment [1–5]. The OC is the deadliest malignant cancer which includes more than 225,000 new patients annually [6]. Due to the late diagnosis of the disease, more than 70% of the patients are in the advanced stage [7]. The well-known oncomarker for the diagnosis of OC in clinics is CA-125, which has been considered the "gold standard" in the last years [8]. CA-125 is a protein with a relatively high molecular weight, and its physiologic amount in the body is less than 35 U/mL [9–11]. Due to the presence of CA-125 on the surface of ovarian tumor cells, its detection by polyclonal antibodies such as anti-CA-125, it can be used to monitor disease progress and also response to chemotherapy [12]. After many studies in the last few years to prove the effectiveness of CA-125 in diagnosing OV, the US

✉ Balal Khalilzadeh
khalilzadehb@tbzmed.ac.ir; balalkhalilzadeh@gmail.com

✉ Rahim Mohammad-Rezaei
r.mohammadrezaei@azaruniv.ac.ir

1 Research Center for Pharmaceutical Nanotechnology, Tabriz University of Medical Sciences, Tabriz, Iran

2 Department of Chemistry, Faculty of Basic Sciences, Azarbaijan Shahid Madani University, Tabriz, Iran

3 Stem Cell Research Center, Tabriz University of Medical Sciences, Tabriz, Iran

4 Hematology and Oncology Research Center, Tabriz University of Medical Sciences, Tabriz, Iran

5 Department of Basic Medical Sciences, Khoy University of Medical Sciences, Khoy, Iran

Food and Drug Administration (FDA) formally confirmed its effectiveness in the initial stage of OC diagnosis [6, 13]. Therefore, there is a great demand for ultrasensitive detection of CA-125 using cost-effective yet robust and more accurate methods. To diagnose this disease, blood cell count tests, tomography scan, ultrasound, and magnetic resonance imaging of the pelvis, laparoscope, and finally tumor biopsy are performed [14–16].

Some of traditional methods for measuring cancer biomarkers required complex protocols and instruments. Therefore, researchers are looking to find a rapid and elective detection method. Some of these methods include enzyme-linked immunosorbent assays (ELISAs), mass spectrometry immunoassays, radioimmunoassays, immunohistochemistry, and fluorescent spectroscopy. Some of the previously discussed methods, not all of them have various limitations when compared to the newly developed methods, for example, low sensitivity and false positive detection in ELISAs, expensive equipment in chemiluminescence, and low selectivity in some of the approaches [17–22].

Electrochemical techniques are a promising strategy due to advantages such as fast response time, good sensitivity, high selectivity, and a precise tool for binding antibody-antigen (Ab-Ag) with high affinity. Therefore, the electrochemical biosensor could be applied as sensitive, fast response time, and selective detection of biomarkers [23].

In recent decades, scientists have investigated biosensors composed with various biomaterials and nanomaterials with various sensing methods for monitor and detect cancer biomarkers [24, 25]. Different nanomaterials such as carbon nanomaterials, graphene and its derivatives, Au nano particles, and magnetic nano particles have been used for the construction of biosensors because of the improvement of conductivity and sensitivity. In many cases, combining nanomaterials and bio identifiers as antibodies, aptamers, and enzymes has brought good results in terms of sensitivity and selectivity. Biomaterials conjugated with bioreceptors have been widely used to the construction of optical biosensors and electrochemical as detector of cancer-specific biomarkers [26–29]. Biochemical process by electrochemical biosensors converts into electrical signals. Antigen–antibody interactions are an example of these events [30]. This method has been used for detecting CA-125 protein by bioconjugation anti-CA-125 antibodies on a graphene-based screen-printed bioassay [31]. Another study employed the quenching ability of AuNPs coated with a Schiff base ligand placed in a sol-gel film [32].

MXene is a group of two-dimensional (2D)-transition metal carbide, nitrile, or carbonitrile of the generic formula $M_{n+1}\ X_n\ T_x$ where *M* represents transition; *X* is either *C* or *N*; *T* indicates the surface terminal group, which makes facilitates absorb biological materials and changes the conductivity properties. Therefore, it can be a suitable and flexible candidate in the sensing of biological materials. So far, electrochemical biosensors based on MXene nanosheet have been used for detecting phenol, antibodies, enzymes, and Geno sensor [33].

Graphene quantum dots (GQDs) are thin layer of graphene smaller than 100 nm that possess various optical and electronic properties, which make it an appropriate candidate for fabricating electronic and optical devices at the nanoscale. Due to its good biocompatibility, low toxicity, and good conductivity, GQDs have been shown to be an efficient biosensor [34, 35].

In the present research, we developed a novel immunosensor based on the affinity of CA-125 antibody and CA-125 antigen using glassy carbon electrodes modified MXene-GQD/AuNPs. The outcomes of this modified electrode revealed simple instrumentation, acceptable sensitivity, and good selectivity to the detection of CA-125 (see Scheme 1). This work proposed an electrochemical immunosensor for the detection of OC using MXene-GQD/AuNPs nanocomposite in real samples.

Experimental

Materials

Hydrofluoric acid solution (HF) (48 wt%), Ti_3AlC_2 powder (size of particles 40–60 µm; ≥99% purity), and dimethyl sulfoxide (DMSO) were purchased from Sigma-Aldrich. Due to the systemic toxicity resulting from the dissociated fluoride ion, personal protective equipment and the fume hood were used. Stock solution was prepared in graphite fine powder, 0.05 molar phosphate buffer solution (PBS, pH=7) and complex $[Fe(CN)_6]^{-3/-4}$ were purchased from Merck. CA-125 and its capture antibody were purchased from Abcam.

Apparatus

To homogenize the solutions, an ultrasonic bath (Transsonic, model) was employed. The scanning electron microscope (FE-SEM) and energy dispersive X-ray analyzer (EDX) was performed using Tescan instrument, Model: MIRA3. All electrochemical studies were performed by applying a Metrohm Autolab (PGSTAT204) controlled by Nova software (2.1). The electrochemical three-electrode system consists of a 2-mm diameter glassy carbon electrode (GCE) modified with MXene-GQD/AuNPs as the working electrode, a platinum wire as the counter electrode, and a saturated Ag/AgCl reference electrode.

The synthesis of GQDs [35], AuNPs [36], and MXene [37] is described in Electronic Supporting Material (ESM).

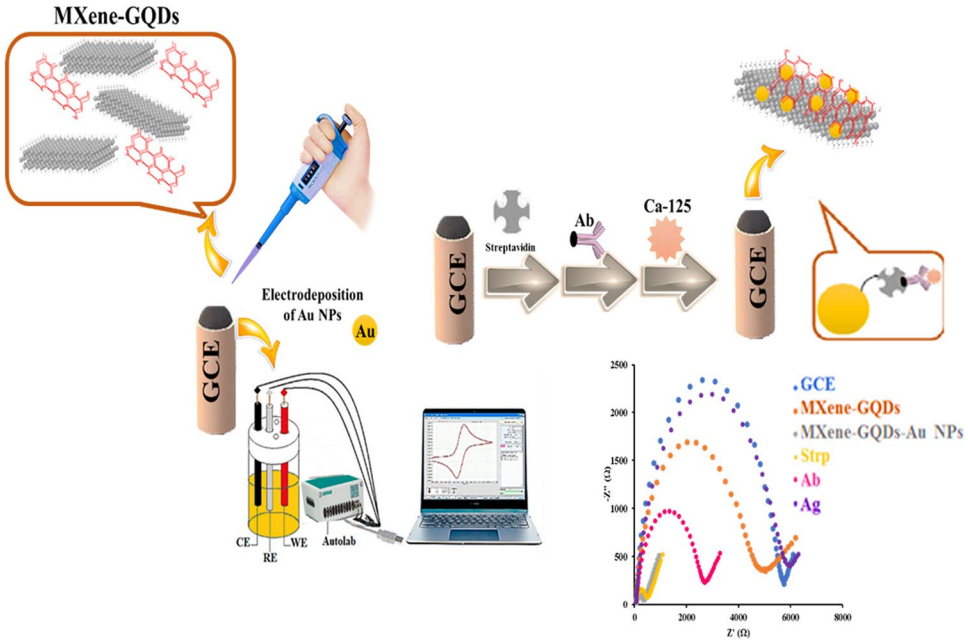

Scheme 1 Scheme of the suggested immunosensor for detection of CA-125

Results and discussion

Electrochemical characterization and statistical analysis

The mentioned electrochemical studies were performed in the mixture of 0.1 M KCl and 5 mM $[Fe(CN)_6]^{-3/-4}$ solution. Also, for statistical analysis, each experiment was repeated ten or more times to obtain the mean±standard deviation (SD) expressed as the mean.

Fabrication of the immunosensor for CA-125

At first, GCE was polished with Al_2O_3 grout to make it mirror-like, and ultrasonic rinsing was performed in 50% HNO_3, 95% C_2H_5OH, and high-purity water for 10 min and dried. With a modified working electrode in $[Fe(CN)_6]^{-3/-4}$ solution, the electrochemical proficiency of each step was investigated by cyclic voltammetry (CV) technique.

At first, 2 mL of 0.1 mg/mL MXene and 2 mL of 0.1 mg/mL GQDs were stirred regularly for 120 min then sonicated for 60 min. Four microliters of the mixture was dripped onto the GCE electrode and dried at room temperature. Thenceforth, AuNPs were electrochemically deposited on the MXene-GQDs by chronoamperometry technique (−0.2 V, 300 s). Gold NPs improved the absorption and increased the effective surface area performance of GCE. In Fig. 1A, CV and Fig. 1B, EIS of the bare GCE, MXene-GQD and MXene-GQD/AuNPs are presented. By the modification surface of GCE with MXene-GQD/AuNPs, currents of CV peaks increased and electron transfer resistance decreased compared with unmodified GCE. The bare electrode showed a charge transfer resistance (R_{ct}) of 5665.97 Ω, and the modified electrode showed R_{ct}=322.15 Ω due to its high conductivity.

Next, the modified GCE electrode (MXene-GQD/AuNPs) was incubated with 2 µL of 0.001 µg/mL streptavidin (Strp, streptavidin is commonly used as a bioconjugation agent in immunoassay) solution at 8 °C. After that, 2 µL of 0.001 µg/mL CA-125 antibody was drop-casted onto Strp-MXene-GQD/AuNPs (Ab-Strp-MXene-GQD/AuNPs) and incubated at 8 °C for 2 h. Eventually, 2 µL CA-125 antigen solution was dropped on the modified GCE and retained at 8 °C for 2 h. Unbound materials were washed with a phosphate buffer with pH 7. As shown in Fig. 1C, CV peaks were generated in variant immunosensor preparation steps of adding Strp, Ab, and Ag (CA-125); currents of CV peaks were reduce, which is because of the prevention of electron transfer on the surface of GCE by CA-125 antibodies and antigens. Figure 1D shows the EIS spectra of the prepared immunosensor. As can be seen, by adding Strp, Ab, and Ag (non-conducting CA-125), the electron transfer resistance increased gradually which can be utilized as a proper analytical signal for ovarian cancer detection.

Morphology and characterization

Scanning electron microscopy (SEM) was used for the evaluation of the morphology of the fabricated immunosensor. As shown in Fig. 2A–D in the nanoscale (with magnified 500 nm, 1 µm, 2 µm, and 5 µm), the

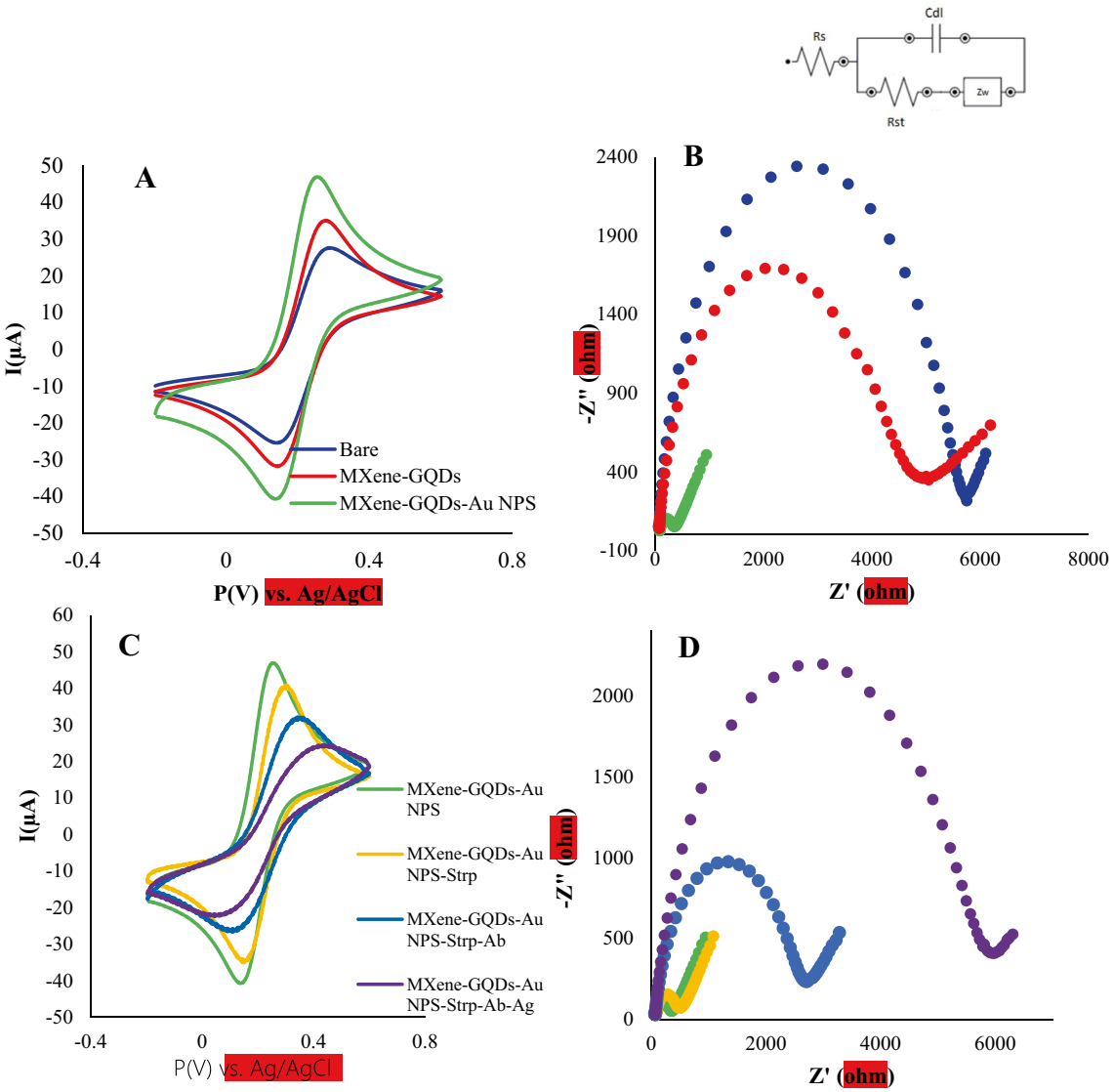

Fig. 1 Verification of electrochemical performance: CV (**A**) and EIS (**B**) of bare GCE, MXene-GQDs, and MXene-GQD/AuNPs. Immunosensor preparation steps: CV (**C**) and EIS (**D**) of MXene-GQDs-AuNPs, MXene-GQD/AuNPs-Strp, MXene-GQD/AuNPs-Strp-Ab, and MXene-GQD/AuNPs-Strp-Ab-Ag in 0.1 M KCl and 5 mM $[Fe(CN)_6]^{-3/-4}$ (0.05 V s^{-1})

FE-SEM, results presented fragmented and frizzly GQD sheets on the surface of the GCE, was produced. Also, the MXene had a dense multilayer sheet, an accordion-like shape, and the surface of MXene was smooth and flat. This morphology of MXene is related to the etching process. The etched sample of $Mn^{+1}AXn$ parent phases was successfully expanded with Al, and multilayer Ti_2CTx was obtained [38]. Therefore, the multilayer MXene provides a wide specific surface area for a lot of Au nanoparticle attachments.

The FE-SEM images of the MXene-GQD/AuNPs-GCE in the nanoscale (with magnified 500 nm, 1 µm, 2 µm, and 5 µm) represent AuNP nanostructures in the deposited matrix in electrodes (Fig. 2E–H). The modified surfaces have different structure and morphology, which reveals the successful deposition of AuNP nanocomposite. Therefore, the deposition of AuNPs was successfully carried out on layered MXene-GQDs.

The energy dispersive X-ray spectroscopy (EDS) provides insight into the chemical compositions of MXene-GQD/AuNPs. The EDS analysis confirms the presence of carbon (C) and titanium (Ti) elements, which can be attributed to the MXene. The presence of oxygen (O) and carbon (C) can be attributed to the GQDs. Moreover, the presence of gold (Au) element after the electrochemical deposition of Au NPs can be confirmed (Fig. 2I).

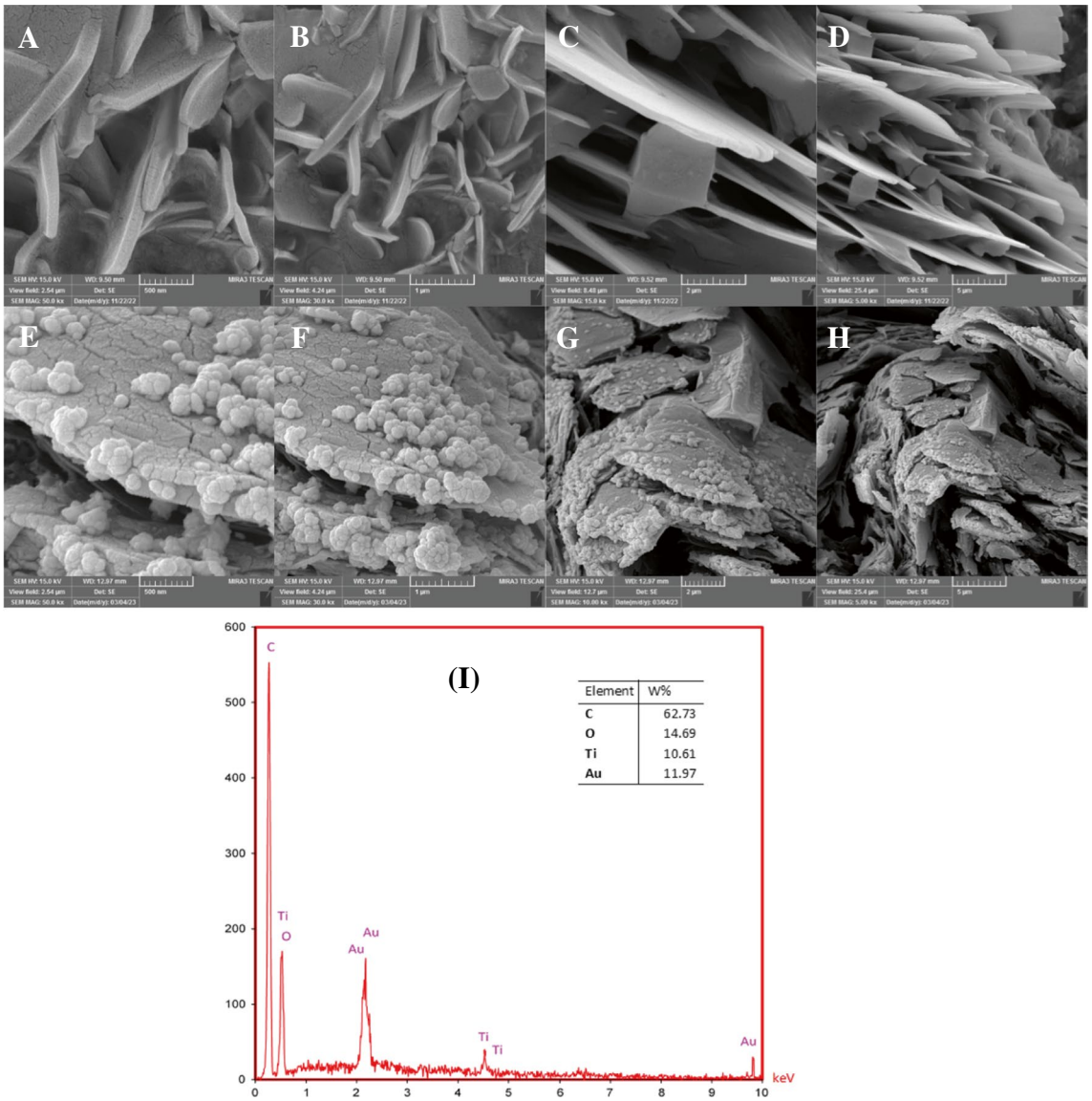

Fig. 2 Description of scanning electron microscopy images in the nanoscale (with magnified 500 nm, 1 µm, 2 µm, and 5 µm): (**A–D**) MXene-GQDs-GCE and (**E–H**) MXene-GQD/AuNPs-GCE. (**I**) Description of MXene-GQD/AuNPs EDS

Optimization of experimental conditions

Optimization of MXene-graphene quantum dot thickness on GCE

Initially, the concentration of MXene-GQDs nanocomposites on the surface of GCE was optimized by different volumes (2, 4, 6, 8, and 10 µL) of MXene-GQD suspension onto the clean GCE. After drying the modified MXene-GQD electrodes for 2 h at room temperature, the electrochemical activity of modified MXene-GQDs electrodes in $[Fe(CN)_6]^{-3/-4}$ solution was evaluated through the CV technique in the potential range of −0.2 to + 0.6 V and also the scanning speed of 50 mV s^{-1} (10 cycles) (Fig. S1A). The average height of the recorded peaks corresponding to each calculated volume and the histogram of average peak height versus different applied volumes of MXene-GQDs presented that the volume of 4 µL is the optimal volume of MXene-GQDs (Fig. S1B).

It must be noted that any increase in the thickness of the resulting layers could hinder redox reaction on the electrode or insulating agent or be a semiconductor. Finally, to optimize incubation time, MXene-GQD electrodes were incubated for 60, 90, 120, and 150 min. According to the obtained voltammograms, the optimum incubation time was 120 min (Fig. S2A and B).

Gold nanoparticles were used to improve the conductivity of the MXene-GQDs as bioconjugation elements on the

surface of the modified electrode. According to the impedance spectra results, the bare electrode showed R_{ct}=5665.97 Ω, MXene-GQDs showed R_{ct}=4908.7 Ω, and MXene-GQD/AuNPs electrode showed R_{ct}=322.15 Ω due to its high conductivity. In fact, the charge transfer resistance with the modified electrode is reduced due to the increase in the conductivity of the electrode surface (Fig. S3A). According to Fig. S3B, the recorded results indicate that the electrochemical performance demonstrates a satisfactory level of stability among 9 days.

Active surface area calculations

Figure 3 shows the relevant CVs of the MXene-GQD/AuNP-modified electrode at different scan rates of 10–500 mV/s to examine the sensing kinetics. According to Fig. 3A, at higher scan rates, one can observe an increase in the width of the voltammograms, along with a rise in both the cathodic and anodic peak currents. The increase in peak current intensity is related to two variables: (I) the scan rate and (II) the square root of the scan rate [39–41]. Figure 3B shows the relationship that changes proportionally of Ip versus $\upsilon^{1/2}$. Based on the recorded results, the diffusion process controls the mass-transferring phenomenon in this study. As a result, the subsequent Randles-Sevcik equation can be used to clarify the electrochemical procedure:

$$I_p = 2.69 \times 10^5 \times AD^{1/2}n^{3/2}C\upsilon^{1/2} \quad (1)$$

In Eq. 1, I_p represents the anodic peak current, C represents the concentration of $[Fe(CN)_6]^{3-/4-}$ (5 mM), n is the number of transferred electron (n=1), A represents the surface area (cm^2), υ denotes the scan rate, and D which is equal to 0.76×10^{-5} cm^2/s confirms the diffusion coefficient. Based on the gained slope of the Ip vs. $\upsilon^{1/2}$ plot, the surface area of modified GCE was calculated as 0.0637 cm^2 (Fig. 3).

Analytical studies

Calibration plots of the optimized system were taken in the different concentrations of CA-125 antigen (0.1, 0.2, 0.4, 0.6, 0.8, and 1 nU/mL) 10 times for each concentration and in the range of −0.2 to 0.6 V. According to the SWV responses shown in Fig. 4, SWV voltammograms are decreased by increasing the concentration of CA-125 that provide high sensitivity for CA-125 detection. The results showed an appropriate linear relationship between the SWV response and the concentrations of CA-125 (linear range 0.1–1 nU/mL), and the detection limit of the CA-125 antigen as an ovarian cancer biomarker for the designed immunosensor was 0.075 nU/mL (S/N=3).

Table 1 provides a comparison between the proposed protocol with other reported immunosensor for the detection of CA-125. In a study [42], a sandwich electrochemiluminescence (ECL) immunosensor was used to detect CA-125 with the Ru-AuNPs/GR labeled, and the detection limit was 0.005 U/mL. In 2014, an electrochemiluminescence immunosensor including a paper electrode containing silver modified with silica NPs and activated with carbon dots showed a limit of detection of 4.3 mU/mL for CA-125 [43]. For tumor marker detection, a sandwich sensor of CdTe quantum dot coated with carbon microspheres and a gold-silver composite as the sensing platform with the detection limit of 2.5 mU/mL were used [44]. In another report, a modified electrode with poly (3-hydroxyphenylacetic acid) was developed to evaluate tumor marker interactions. This sensor provides a detection limit of 1.45 U/mL [45]. In a study, a printed carbon electrode was used to design an immunosensor based on g-C_3N_4. This sensor was chemically prepared by binding antigen with g-C_3N_4 with its detection limit of 0.4 mU/mL [46].

Based on the results discussed (Table 1), the analytical properties of the suggested sensing assay have been improved in comparison to prior studies. The heightened

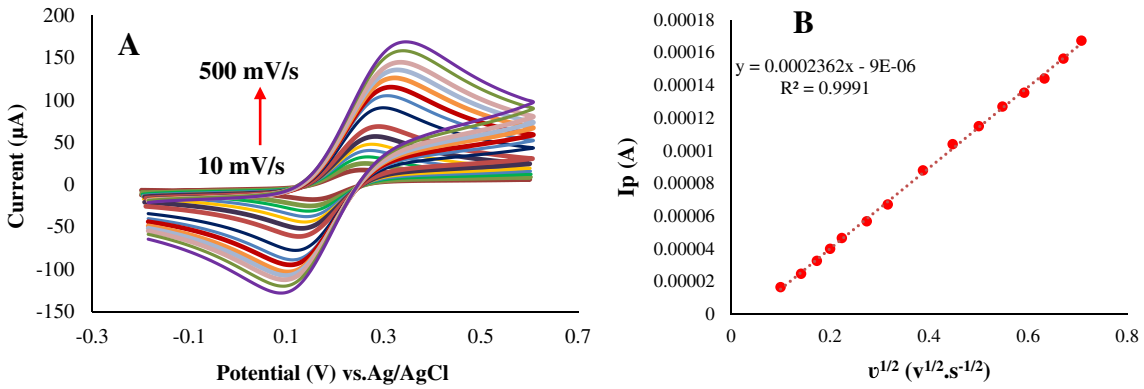

Fig. 3 **A** CVs of MXene-GQD/AuNP GCE in $[Fe(CN)_6]^{3-/4-}$ (5 mM) in different scan rates (10, 20, 30, 40, 50, 75, 100, 150, 200, 250, 300,350, 400, 450, and 500 mV/s) and **B** I_p (µA) vs. ($V^{1/2}$ /$s^{1/2}$)

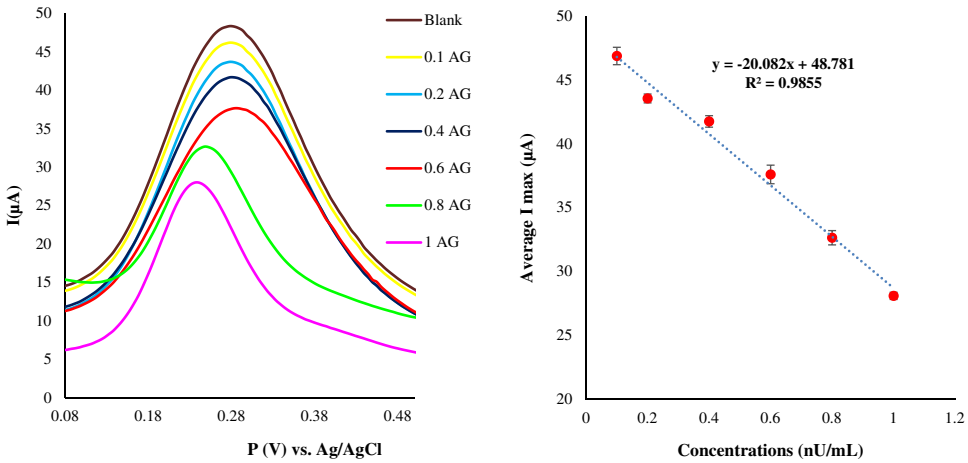

Fig. 4 The SWV responses by increasing the concentration of CA-125 (0.1, 0.2, 0.4, 0.6, 0.8, and 1 nU/mL) and calibration plot at different CA-125 concentrations in 0.1 KCl containing 5 mM $[Fe(CN)_6]^{-3/-4}$ (0.05 V s^{-1})

Table 1 Provides a comparison between proposed protocol with other reported immunosensors for the detection of CA-125

Platform	LOD	Linear range	Reference
Ru-AuNPs/GR	5 mU/mL	0.01–100 U/mL	[42]
Amino-modified silica NPs	4.3 mU/mL	0.01–50 U/mL	[43]
Au-Ag nanocomposite-modified graphene	2.5 mU/mL	0.008–50 U/mL	[44]
Poly (3-hydroxyphenylacetic acid)	1450 mU/mL	5–80 U/mL	[45]
Multi-functionalized g-C3N4	0.4 mU/mL	0.001–5 U/mL	[46]
CuCo-ONSs@AuNPs	3.9×10^{-8} U/mL	10^{-7}–10^{-3} U/mL	[47]
A gold–vertical graphene/TiO_2	0.0001 mU/mL	0.01–1000 mU/mL	[48]
AuNP/RGO	0.000042 U/mL	0.0001–300 U/mL	[49]
MXene-GQD/AuNPs	0.075 nU/mL	0.1–1 nU/mL	This work

sensitivity of the proposed immunosensor can be attributed to the incorporation of MXene-GQD/AuNPs, which possess a high electron transfer rate and abundant active sites. These properties facilitate the enhanced immobilization of antibodies, thereby improving the efficiency of antibody-antigen binding and increasing the available surface area. Consequently, the obtained results indicate that the developed bioassay offers a viable immunosensor for the precise detection of CA-125 at minimal concentrations.

Selectivity, stability, reproducibility, and repeatability of the designed immunosensor

The reproducibility of the immunosensor was evaluated in the presence of 0.1 nU/mL CA-125 antigen with three different MXene-GQD/AuNPs-GCE which were independently prepared, and the average peak height of 10 successive measurements was calculated. The result showed that the relative standard deviation (RSD) was obtained to measure the reproducibility of 2.04%. To evaluate the repeatability of the engineered immunosensor, three antigen concentrations of 0.1, 0.6, and 1 nU/mL were selected and modified in three different GCE electrodes separately. The resulting DPV voltammograms (recorded 10 times under the same conditions) showed that the immunosensor has suitable repeatability. To study the stability of the prepared immunosensor, the modified Ab-Strp-(MXene-GQD/AuNPs) electrode was kept at 8 °C from 1 to 4 days, and then the voltammogram of the electrode was taken in 0.1 KCl containing 5 mM $[Fe(CN)_6]^{-3/-4}$ (0.05 V s^{-1}), which showed that after 4 days, 2% reduction in DPV is observed Fig. S4. No significant alteration in the electrochemical signal was displayed after 4-day storing; also after performing the electrode preparation steps, 1 µL of antigen (0.4 nU/mL) was examined, and voltammogram was recorded 10 times. Then, capped on the final modified electrode, it was kept at 4 °C. One-hundred twenty hours later, five SWV voltammograms recorded in the same conditions showed that the average peak height of SWV voltammogram decreased approximately by 15% compared to the first day. To evaluate the selectivity of the developed immunosensor, PSA (1 nU/mL), CA-15-3 (1 nU/mL), and CA-19-9 (1 nU/mL), a mixture solution included PSA, CA-15-3, and CA-19-9 (1 nU/mL), and CA-125 (0.5 nU/mL) was used as an interfering material. Figure S5A, B confirms that the electrochemical signal of the immunosensor was stable in the presence or absence of these interfering compounds, which indicates the high selectivity of the immunosensor .

Table 2 Addition and determination of CA-125 in real healthy samples with the MXene-GQD/AuNPs immunosensor (n=6)

No	Added (nU/mL)	Found (nU/mL)	Recovery
1	0	0	-
2	0.1	0.0981	98.1%
3	0.2	0.211	105%
4	0.4	0.401	100%
5	0.6	0.618	103%
6	0.8	0.825	103%
7	1	1.01	101%

Applicability of the immunosensor in analyzing real samples

The prepared immunosensor was applied for the quantification of CA-125 in the diluted serum samples with 10 mL PBS (pH=7). Various concentrations of the CA-125 antigen were added to diluted samples (Table 2). Then, 2 µL of treated serum sample with the CA-125 at the 0.1, 0.2, 0.4, 0.6, 0.8, and 1 nU/mL concentration levels was immobilized on MXene-GQD/AuNPs-GCE. The results of the SWV technique are shown in Fig. 5. The recoveries which ranged from 98.1 to 105% were obtained for the real samples. Accordingly, there is no difference between the electrical signal of the healthy person sample and the modified electrode without antigen CA-125. Additionally, the developed immunosensor was desirably applied for the evaluation of CA-125 in ovarian cancer suffering patient's serum samples at two different stages and healthy sample (the results are presented in Fig. S6A, B).

These results indicated that the proposed electrode has a good application due to the advantages shown in the production and identification stages. Future work should focus on developing new portable tools with the advantages of our proposed platform that will bring benefits for point-of-care diagnostics in clinical settings.

Conclusion

In this project, a label-free biosensor with desirable sensitivity was developed for the evaluation of CA-125. Hence, MXene-GQD/AuNPs, immobilized on the working electrode as an effective mediator, enhance the active surface area of the modified GCE and increase the stability and conductivity of the bioassay system. Similarly, AuNPs existent in the nanocomposition of the modifying agent not only helped to intensify the electron transfer rate, but also led to the effective bioconjugation of anti-CA-125 on the modified electrode. The presented bioassay showed high efficacy in the ultrasensitive evaluation of CA-125 with desirable LOD, venerable selectivity, and long-term stability. The ultrasensitive methods could help physicians to quickly change the therapeutic strategy by prescribing the different drugs for efficient treatment outcomes. However, the limitations of the designed immunosensor are associated with incubation time. Also, our linear range is narrow, it will be desirable if we can increase our linear range in future works. Due to the described advantages, the prepared biosensor could serve as a promising tool for ultrahigh-sensitive detection of other cancerous biomarkers. As a result, we believe that there will be notable advancements in the development of nano-based sensing devices for therapeutic purposes, aligning with diagnostic applications across different fields in the near future.

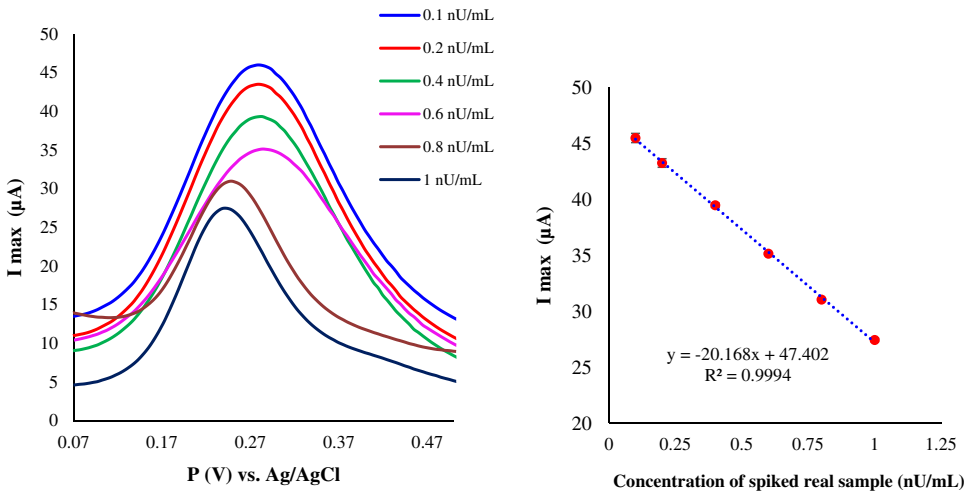

Fig. 5 SWV results of the CA-125 addition and determination in real healthy samples with the MXene-GQD/AuNPs immunosensor (n=6)

Supplementary Information The online version contains supplementary material available at https://doi.org/10.1007/s00604-024-06469-z.

Acknowledgements The authors gratefully thank the Stem Cell Research Center for financial support and also gratefully acknowledge the Azarbaijan Shahid Madani University for the support.

Author contribution Zahra Hosseinchi Gharehaghaji contributed in all experimental analysis and preparing the first draft. Balal Khalilzadeh supervised the study and participated in idea, development of the method, validation of data, and editing. Hadi Yousefi helped in validation of data and editing. Rahim Mohammad-Rezaei supervised the study and assisted data interpretations and editing.

Funding This project was financially supported by the Stem Cell Research Center, Tabriz University of Medical Sciences, Tabriz, Iran (grant no. 71958).

Data availability Not applicable.

Declarations

Ethics approval and consent to participate All patients were asked to complete the informed consent. All procedures of this study were approved by the Local Ethics Committee of Tabriz University of Medical Sciences (IR.TBZMED.REC.1402.255). All procedures were done under the Declaration of Helsinki.

Conflict of interest The authors declare no competing interests.

References

1. Chandra A, Pius C, Nabeel M, Nair M, Vishwanatha JK, Ahmad S, Basha R (2019) Ovarian cancer: current status and strategies for improving therapeutic outcomes. Cancer Med 8(16):7018–7031
2. Gupta KK, Gupta VK, Naumann RW (2019) Ovarian cancer: screening and future directions. Int J Gynecologic Cancer 29 (1)
3. Keshavarz M, Tan B, Venkatakrishnan K (2018) Multiplex photoluminescent silicon nanoprobe for diagnostic bioimaging and intracellular analysis. Adv Sci 5(3):1700548
4. Lheureux S, Gourley C, Vergote I, Oza AM (2019) Epithelial ovarian cancer. Lancet 393(10177):1240–1253
5. Karimzadeh Z, Hasanzadeh M, Isildak I, Khalilzadeh B (2020) Multiplex bioassaying of cancer proteins and biomacromolecules: nanotechnological, structural and technical perspectives. Int J Biol Macromol 165:3020–3039
6. De La Franier B, Thompson M (2019) Early stage detection and screening of ovarian cancer: a research opportunity and significant challenge for biosensor technology. Biosens Bioelectron 135:71–81
7. Katchman BA, Chowell D, Wallstrom G, Vitonis AF, LaBaer J, Cramer DW, Anderson KS (2017) Autoantibody biomarkers for the detection of serous ovarian cancer. Gynecol Oncol 146(1):129–136
8. Yuan J, Duan R, Yang H, Luo X, Xi M (2012) Detection of serum human epididymis secretory protein 4 in patients with ovarian cancer using a label-free biosensor based on localized surface plasmon resonance. International journal of nanomedicine:2921–2928
9. Charkhchi P, Cybulski C, Gronwald J, Wong FO, Narod SA, Akbari MR (2020) CA125 and ovarian cancer: a comprehensive review. Cancers 12(12):3730
10. Dochez V, Caillon H, Vaucel E, Dimet J, Winer N, Ducarme G (2019) Biomarkers and algorithms for diagnosis of ovarian cancer: CA125, HE4, RMI and ROMA, a review. J Ovarian Res 12:1–9
11. Zhang M, Cheng S, Jin Y, Zhao Y, Wang Y (2021) Roles of CA125 in diagnosis, prediction, and oncogenesis of ovarian cancer. Biochimica et Biophysica Acta (BBA)-Reviews on Cancer 1875(2):188503
12. Sharma SK, Suresh MR, Wuest FR (2014) Improved soluble expression of a single-chain antibody fragment in E. Coli for targeting CA125 in epithelial ovarian cancer. Protein Exp Purif 102:27–37
13. Bottoni P, Scatena R (2015) The role of CA 125 as tumor marker: biochemical and clinical aspects. Advances in Cancer Biomarkers: From biochemistry to clinic for a critical revision:229–244
14. Dolati S, Soleymani J, Shakouri SK, Mobed A (2021) The trends in nanomaterial-based biosensors for detecting critical biomarkers in stroke. Clin Chim Acta 514:107–121
15. Hong R, Sun H, Li D, Yang W, Fan K, Liu C, Dong L, Wang G (2022) A review of biosensors for detecting tumor markers in breast cancer. Life 12(3):342
16. Olejnik B, Kozioł A, Brzozowska E, Ferens-Sieczkowska M (2021) Application of selected biosensor techniques in clinical diagnostics. Expert Rev Mol Diagn 21(9):925–937
17. Abolhasan R, Khalilzadeh B, Yousefi H, Samemaleki S, Chakari-Khiavi F, Ghorbani F, Pourakbari R, Kamrani A, Khataee A, Rad TS (2021) Ultrasensitive and label free electrochemical immunosensor for detection of ROR1 as an oncofetal biomarker using gold nanoparticles assisted LDH/rGO nanocomposite. Sci Rep 11(1):14921
18. Dezhakam E, Khalilzadeh B, Mahdipour M, Isildak I, Yousefi H, Ahmadi M, Naseri A, Rahbarghazi R (2023) Electrochemical biosensors in exosome analysis; a short journey to the present and future trends in early-stage evaluation of cancers. Biosens Bioelectron 222:114980
19. Jalili R, Chenaghlou S, Khataee A, Khalilzadeh B, Rashidi M-R (2022) An electrochemiluminescence biosensor for the detection of Alzheimer's tau protein based on gold nanostar decorated carbon nitride nanosheets. Molecules 27(2):431
20. Nasrollahpour H, Khalilzadeh B, Hasanzadeh M, Rahbarghazi R, Estrela P, Naseri A, Tasoglu S, Sillanpää M (2023) Nanotechnology-based electrochemical biosensors for monitoring breast cancer biomarkers. Med Res Rev 43(3):464–569
21. Nasrollahpour H, Khalilzadeh B, Naseri A, Yousefi H, Erk N, Rahbarghazi R (2022) Electrochemical biosensors for stem cell analysis; applications in diagnostics, differentiation and follow-up. TRAC Trends Anal Chem 156:116696
22. Nasrollahpour H, Naseri A, Rashidi M-R, Khalilzadeh B (2021) Application of green synthesized WO3-poly glutamic acid nanobiocomposite for early stage biosensing of breast cancer using electrochemical approach. Sci Rep 11(1):23994
23. Ravalli A, Dos Santos GP, Ferroni M, Faglia G, Yamanaka H, Marrazza G (2013) New label free CA125 detection based on gold nanostructured screen-printed electrode. Sens Actuators B 179:194–200
24. Huang X, Zhu Y, Kianfar E (2021) Nano biosensors: properties, applications and electrochemical techniques. J Mater Res Technol 12:1649–1672
25. Sivasankarapillai VS, Somakumar AK, Joseph J, Nikazar S, Rahdar A, Kyzas GZ, Nano-Structures (2020) Cancer theranostic applications of MXene nanomaterials: recent updates. Nano-Structures & Nano-Objects 22:100457
26. Mehrannia L, Khalilzadeh B, Rahbarghazi R, Milani M, Saydan Kanberoglu G, Yousefi H, Erk N (2023) Electrochemical biosensors as a novel platform in the identification of listeriosis infection. Biosensors 13(2):216

27. Mirzaie A, Nasrollahpour H, Khalilzadeh B, Jamali AA, Spiteri RJ, Yousefi H, Isildak I, Rahbarghazi R (2023) Cerebrospinal fluid: a specific biofluid for the biosensing of Alzheimer's diseases biomarkers. TrAC Trends in Analytical Chemistry:117174
28. Nasrollahpour H, Khalilzadeh B (2023) Naked eye biosensors for pathogen monitoring. TRAC Trends Anal Chem :117499
29. Nasrollahpour H, Mirzaie A, Sharifi M, Rezabakhsh A, Khalilzadeh B, Rahbarghazi R, Yousefi H, Klionsky DJ (2024) Biosensors; a novel concept in real-time detection of autophagy. Biosens Bioelectron :116204
30. Cho I-H, Kim DH, Park S (2020) Electrochemical biosensors: perspective on functional nanomaterials for on-site analysis. Biomaterials Res 24(1):1–12
31. Sawhney MA, Conlan R (2019) POISED-5, a portable on-board electrochemical impedance spectroscopy biomarker analysis device. Biomed Microdevices 21:1–14
32. Abou-Omar MN, Attia MS, Afify HG, Amin MA, Boukherroub R, Mohamed EH (2021) Novel optical biosensor based on a nano-gold coated by Schiff base doped in sol/gel matrix for sensitive screening of oncomarker CA-125. ACS Omega 6(32):20812–20821
33. Xu B, Zhi C, Shi P (2020) Latest advances in MXene biosensors. J Physics: Mater 3(3):031001
34. Razmi H, Mohammad-Rezaei R (2013) Graphene quantum dots as a new substrate for immobilization and direct electrochemistry of glucose oxidase: application to sensitive glucose determination. Biosens Bioelectron 41:498–504
35. Soleimanian A, Khalilzadeh B, Mahdipour M, Aref AR, Kalbasi A, Bazaz SR, Warkiani ME, Rashidi MR, Mahdavi M (2021) An efficient graphene quantum dots-based electrochemical cytosensor for the sensitive recognition of CD123 in acute myeloid leukemia cells. IEEE Sens J 21(15):16451–16463
36. Pourakbari R, Yousefi M, Khalilzadeh B, Irani-nezhad MH, Khataee A, Aghebati-Maleki L, Soleimanian A, Kamrani A, Chakari-Khiavi F, Abolhasan R (2022) Early stage evaluation of colon cancer using tungsten disulfide quantum dots and bacteriophage nano-biocomposite as an efficient electrochemical platform. Cancer Nanotechnol 13(1):1–17
37. Thirumal V, Yuvakkumar R, Kumar PS, Ravi G, Keerthana S, Velauthapillai D (2022) Facile single-step synthesis of MXene@ CNTs hybrid nanocomposite by CVD method to remove hazardous pollutants. Chemosphere 286:131733
38. Ng VMH, Huang H, Zhou K, Lee PS, Que W, Xu JZ, Kong LB (2017) Recent progress in layered transition metal carbides and/or nitrides (MXenes) and their composites: synthesis and applications. J Mater Chem A 5(7):3039–3068
39. Hasanzadeh M, KARIM-NEZHAD G, Shadjou N, Khalilzadeh B, Saghatforoush L, Ershad S, Kazeman I (2009) Kinetic study of the electro-catalytic oxidation of hydrazine on cobalt hydroxide modified glassy carbon electrode. Chin J Chem 27(4):638–644
40. Saghatforoush L, Hasanzadeh M, Karim-Nezhad G, Ershad S, Shadjou N, Khalilzadeh B, Hajjizadeh M (2009) Kinetic study of the electrooxidation of mefenamic acid and indomethacin catalysed on cobalt hydroxide modified glassy carbon electrode. Bull Korean Chem Soc 30(6):1341–1348
41. Shafaei S, Akbari Nakhjavani S, Kanberoglu GS, Khalilzadeh B, Mohammad-Rezaei R (2022) Electrodeposition of cerium oxide nanoparticles on the graphenized carbon ceramic electrode (GCCE) for the sensitive determination of isoprenaline in human serum by differential pulse voltammetry (DPV). Anal Lett 55(15):2418–2435
42. Li M, Zhang M, Ge S, Yan M, Yu J, Huang J, Liu S (2013) Ultrasensitive electrochemiluminescence immunosensor based on nanoporous gold electrode and Ru-AuNPs/graphene as signal labels. Sens Actuators B 181:50–56
43. Liu W, Ma C, Yang H, Zhang Y, Yan M, Ge S, Yu J, Song X (2014) Electrochemiluminescence immunoassay using a paper electrode incorporating porous silver and modified with mesoporous silica nanoparticles functionalized with blue-luminescent carbon dots. Microchim Acta 181:1415–1422
44. Zhang Y, Li L, Yang H, Ding Y-n, Su M, Zhu J, Yan M, Yu J, Song X (2013) Gold–silver nanocomposite-functionalized graphene sensing platform for an electrochemiluminescent immunoassay of a tumor marker. RSC Adv 3(34):14701–14709
45. de Castro ACH, Alves LM, Siquieroli ACS, Madurro JM, Brito-Madurro AG (2020) Label-free electrochemical immunosensor for detection of oncomarker CA125 in serum. Microchem J 155:104746
46. Wu L, Sha Y, Li W, Wang S, Guo Z, Zhou J, Su X, Jiang X (2016) One-step preparation of disposable multi-functionalized g-C3N4 based electrochemiluminescence immunosensor for the detection of CA125. Sens Actuators B 226:62–68
47. Mu W, Wu C, Wu F, Gao H, Ren X, Feng J, Miao M, Zhang H, Chang D, Pan H (2024) Ultrasensitive and label-free electrochemical immunosensor for the detection of the ovarian cancer biomarker CA125 based on CuCo-ONSs@ AuNPs nanocomposites. J Pharm Biomed Anal 243:116080
48. Chen Z, Li B, Liu J, Li H, Li C, Xuan X, Li M (2022) A label-free electrochemical immunosensor based on a gold–vertical graphene/TiO2 nanotube electrode for CA125 detection in oxidation/reduction dual channels. Microchim Acta 189(7):257
49. Sangili A, Kalyani T, Chen S-M, Nanda A, Jana SK (2020) Label-free electrochemical immunosensor based on one-step electrochemical deposition of AuNP-RGO nanocomposites for detection of endometriosis marker CA 125. ACS Appl Bio Mater 3(11):7620–7630